INTERNATIONAL JOURNAL OF ENERGY STUDIES

e-ISSN: 2717-7513 (ONLINE); homepage: https://dergipark.org.tr/en/pub/ijes

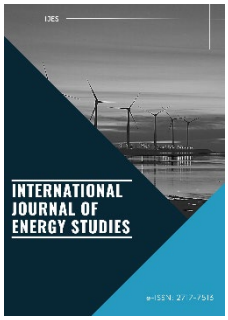

Research Article
Int J Energy Studies 2025; 10(1): 1185-1202
DOI: 10.58559/ijes.1632282

Received : 04 Feb 2025
Revised : 12 Feb 2025
Accepted : 18 Feb 2025

Numerical investigation of in-cylinder swirl motion under cold start conditions in a diesel engine

Fatih Aktas[a*], Zeynep Aytac Yilmaz[b], Nuri Yucel[c]

[a]Gazi University, Department of Mechanical Engineering and Faculty of Engineering, Ankara, Türkiye, ORCID: 0000-0002-1594-5002
[b]Gazi University, Department of Mechanical Engineering and Faculty of Engineering, Ankara, Türkiye, ORCID: 0000-0003-0717-5287
[c]Gazi University, Department of Mechanical Engineering and Faculty of Engineering, Ankara, Türkiye, ORCID: 0000-0001-9390-5877
*(*Corresponding Author: fatihaktas@gazi.edu.tr)*

Highlights

- This study investigates swirl within a diesel engine numerically under cold starting conditions for various valve opening configurations.
- Increased valve openings significantly affect the swirl intensity within the cylinder.
- Excessive swirl can lead to higher heat transfer rates to the cylinder walls and potential flame propagation issues.

You can cite this article as: Aktas F, Aytac Yilmaz Z, Yucel N. Numerical investigation of in-cylinder swirl motion under cold start conditions in a diesel engine. Int J Energy Studies 2025; 10(1): 1185-1202.

ABSTRACT

The performance and efficiency of internal combustion engines, particularly diesel engines, are closely tied to the quality of air-fuel mixing and combustion processes. One of the critical factors influencing these processes is the in-cylinder airflow, specifically the swirl motion, which is the rotational movement of air around the cylinder axis. This swirl plays a pivotal role in enhancing the turbulence required for efficient fuel-air mixing, accelerating flame development, and improving overall combustion. This study shows a numerical analysis of the swirl movement within the cylinder of a diesel engine under cold starting conditions. Using computational fluid dynamics (CFD) analysis, the research evaluates the effects of various valve opening configurations on swirl intensity. Valve openings of 1, 2, 3, 4, 5, and 5.85 mm are analyzed and the results indicate that increasing valve openings generally enhances swirl motion, improving combustion efficiency by promoting better air-fuel mixing. However, excessive swirl can negatively impact performance due to increased heat transfer and potential flame propagation issues. The study also assesses the impact of turbulence models and mesh density on the accuracy of the results, with the k-ε model providing predictions closest to experimental data. These findings contribute to optimizing engine design for improved combustion characteristics and reduced emissions.

Keywords: Cold flow, Swirl motion, Computational fluid dynamics

1. INTRODUCTION

Combustion is basically the chemical interaction of fuel and oxygen [1]. The efficiency of an internal combustion engine is directly related to combustion quality. The combustion quality can be enhanced by improving the homogeneity of the air-fuel mixture along with injection properties or by boosting in-cylinder air swirl intensity [2,3]. Homogeneity or the air swirl intensity depends on turbulence characteristics in cylinder and average velocity field. In order to develop rapid combustion, sufficient amount of turbulence is required at the end of the compression stroke, providing the air and the fuel to mix better and also accelerating the flame development [4]. Also, injection timing is known to be critical in terms of mixture homogeneity [5]. It is known that a better fuel-air mixture plays a crucial role in augmenting the engine performance and combustion characteristics [6]. On the other hand, excessive amount of turbulence can lead to excessive heat transfer from the gases to the cylinder walls and may cause flame propagation problems [7]. It is known that the utilization of CFD tools during the design process provides a deep insight in terms of design, improvements, and optimization [8]. Therefore, simulating these processes with CFD tools is a commonly preferred method as the experimental studies are time and money consuming [9].

In-cylinder air movement in diesel engines is generally characterized by turbulence, compression, and vortex, which have a significant impact on air-fuel mixing and combustion. The vortex motion of the air, as well as its intensity and density, is generally dependent on design of intake port, valve opening, and angular position of valve. A proper intake port design promotes vortex generation and helps optimize combustion [10]. When vortices are present in the in-cylinder air, the vortex-compression interaction produces a complicated turbulent flow field near end of compression, which is significantly more intense in designs with re-entrant combustion chambers [11, 12]. Demirkesen et al. investigated in-cylinder flow field of a diesel engine using both numerical and experimental methods. They found that the numerical and experimental results are in accordance with each other, proving that the numerical method is an efficient way of finding a solution [13]. Huang et al. studied experimentally temporal and spatial processes of flow in a four-valve, four-stroke, single-cylinder, reciprocating motorcycle engine with PIV. The cycle-averaged tumble ratio and turbulence intensity of the engine with the elliptic intake port were larger than those of the engine with the circular intake port, and they discovered that the vortical structures produced by the elliptic intake port were more coherent than those produced by the circular intake port. Measured engine performance was higher having elliptic intake port [14]. Kaplan et al.

numerically investigated the variation of swirl, tumble, turbulence level, and combustion efficiency by using different intake port configurations in a diesel engine. They deduced that the configuration augmenting the swirl ratio and turbulence level does not have an important impact on improving tumble, swirl, and turbulent kinetic energy [15]. Taghavifar et al. carried out a study to determine effect of geometrical modification on piston structure. They discovered that the pressure rises with the bowl's displacement toward the cylinder wall and that smaller bowl sizes improve the chamber's vortex formation [16]. Three-dimensional flow simulations of a four-valve direct-injection diesel engine for various combustion chamber layouts were performed by Payri et al. The findings demonstrated that while bowl form is crucial close to top dead center (TDC) and in the early stages of the expansion stroke, piston geometry has little bearing on in-cylinder flow throughout the intake stroke and the first portion of the compression stroke [17]. Choi et al. simulated the in-cylinder flow of a diesel engine using CFD and presented the results for swirl, tumble, and their influence on turbulent kinetic energy depending on shape, angle, and jet passage area. As a result, they found that flow characteristics were strongly affected by inflow velocity [18]. Jemni et al. used experimental and numerical techniques to investigate how intake manifold design affected in-cylinder flow and engine performance in a diesel engine. They found that the simulation and experiments both prove advantages of the optimized geometry in terms of in-cylinder flow and engine performance [19]. The impact of various piston bowl configurations on in-cylinder flow characteristics was examined by Shafie and Said. They used cold flow analysis to compare in-cylinder flow behaviors for three different piston bowl structures during intake and compression strokes. The results revealed that the variation mentioned does not have a significant effect during intake stroke. However, bowl geometry becomes critical during compression stroke, especially near TDC [20]. Wahono et al. investigated numerically and experimentally the in-cylinder flows of a small motorcycle engine. Using computational fluid dynamics (CFD) methods, authors aimed to analyze the in-cylinder flow characteristics. It was demonstrated that flow coefficient, air flow rate, and discharge coefficient of the numerical and experimental results agree well with one another [21]. Topkaya et al. conducted the numerical analysis of a diesel engine having different combustion chamber bowl geometries. Their results showed that the model with the increased combustion efficiency is the one with the enhanced swirl and the combustion temperature [22].

This study contributes to the literature by numerically investigating the in-cylinder vortex motion under cold start conditions. Although many studies in existing literature have addressed the effects

of different inlet port geometries, piston configurations, or turbulence models on the flow characteristics, this study focuses on the behavior of in-cylinder flow motions during cold start. The complex flow structures resulting from the combination of low temperature and high turbulence under cold start conditions directly impact the engine's efficiency and emission characteristics. This research evaluates the effects of various valve openings on the swirl density with CFD analyses while also revealing the impact of the turbulence models and network structure used on the accuracy of the results. The study results are expected to contribute to developing new strategies to optimize the cold start performance and emission control of diesel engines.

2. THEORY AND METHODOLOGY

2.1. Theory

2.1.1. Swirl number

In a fluid flow cycle, if the fluid is rotating around the cylinder axis, it is referred to as swirl motion; if it is rotating around an axis perpendicular to the cylinder axis, then it is called tumble flow motion. Although tumble motion is not as significant as swirl motion in diesel cycles, it still affects the formation of turbulence. The schematic representation of swirl and tumble motions is given in Figure 1.

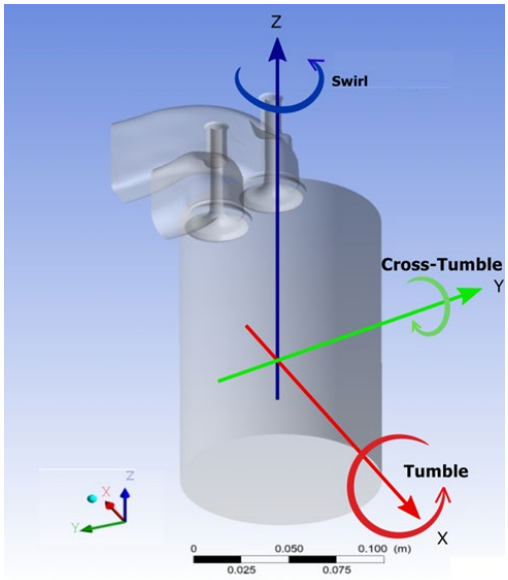

Figure 1. Representation of swirl, tumble, and cross tumble [23]

The magnitude of the swirl motion formed inside the cylinder can be measured experimentally using different methods, and the obtained values can be used to mathematically express the vortex

intensity. Let us consider a swirl flow in a pipe with a radius R, as shown in Figure 2. Here, mass of particle under consideration can be expressed as dm=ρdV. The vector representation of the velocity is given as in Equation 1. Here, U stands for the axial component of velocity, W represents the tangential component of the velocity, i and t denote the unit vectors. The moment of momentum at a random cross-section of the pipe with respect to the X-axis is expressed as in Equation 2, where ρ represents fluid density, r is distance, and v is the velocity vector.

$$v = Ui + Wt \tag{1}$$

$$M = \int_A r\, x(\rho U v) dA \tag{2}$$

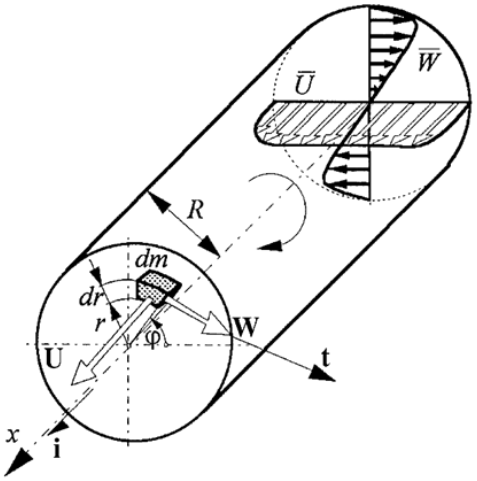

Figure 2. The definition of a swirl flow [24]

In the case of turbulent flow, velocity of the fluid can be written as in Equation 3:

$$v = (\overline{U} + u')i + (\overline{W} + w')t \tag{3}$$

Here, $\overline{U}$ and $\overline{W}$ represent the average velocities, whereas u' and w' represent the fluctuations in velocity components. If Equation 3 is substituted into Equation 2;

$$\overline{M} = \rho \int_A r \times \left[\left(\overline{U}^2 + \overline{u'^2}\right)i + \left(\overline{U}\,\overline{W} + \overline{u'w'}\right)t\right] dA \tag{4}$$

$$\bar{M} = M_x i + M_\varphi t \tag{5}$$

In Equation 5, M_x and M_φ represent the axial and tangential components of the moment, respectively. The swirl number, used in determining vortex density, can be defined as the ratio of the moments generated by the variations in the tangential and axial components of momentum, which can be expressed as in Equation 6.

$$S = \frac{M_\varphi}{M_x} = \frac{\int_A (\bar{U}\bar{W} + \overline{u'w'}) r dA}{R \int_A \left(\bar{U}^2 + \overline{u'^2}\right) dA} \tag{6}$$

If the fluctuation coefficients of velocity resulting from turbulence effects are neglected, the new expression for the swirl ratio can be defined as in Equation 7. Here, V_θ and V_a values represent the tangential and axial velocity components obtained from the computational fluid dynamics analyses.

$$S = \frac{Angular\ Momentum}{Axial\ Momentum} = \frac{\int_A r V_\theta V_a dA}{R \int_A {V_a}^2 dA} \quad or\ S = \frac{\int_0^R V_\theta V_a r^2 dr}{R \int_0^R {V_a}^2 r dr} \tag{7}$$

Swirl and tumble ratios can also be measured using experimental methods under conditions of steady flow. For measurement, the cylinder head is connected to an interchangeable cylindrical tube having the same diameter as the cylinder in the engine. Using the system shown in Figure 3, the air movement (swirl or tumble) produced by air coming in through the intake valve can be measured by the torque value generated on a paddle wheel or honeycomb-shaped plate due to the flow effect.

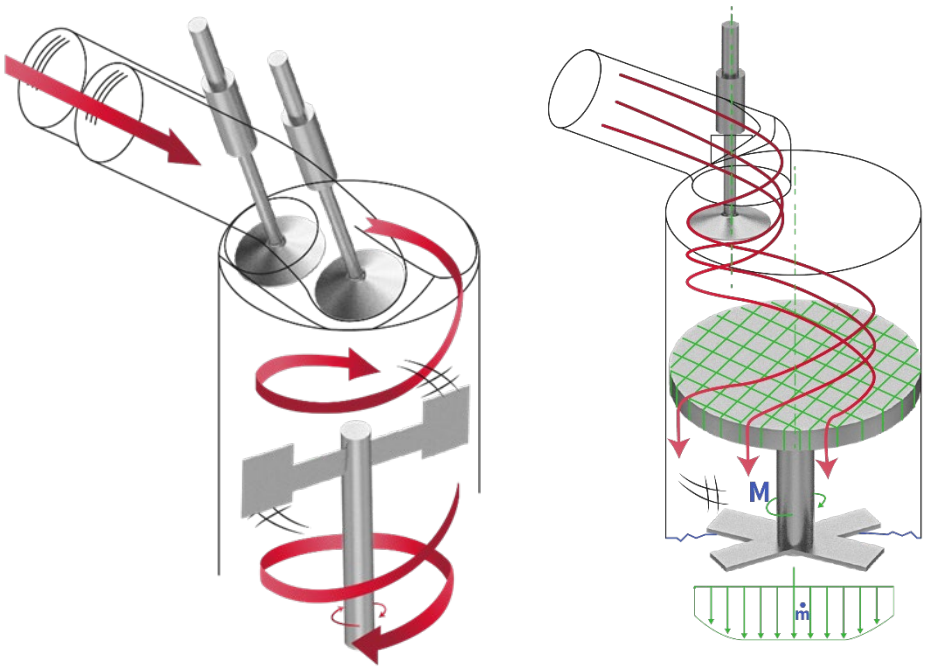

(a)Paddle Wheel (b) Honeycomb

Figure 3. The various measurement methods of swirl motion [25]

2.2. Methodology

Together with experimental studies, computational fluid dynamics (CFD) software is also utilized for optimization of in-cylinder combustion parameters. To enable numerical analyses, it is necessary to introduce the swirl ratio obtained from steady flow apparatus test at the end of the intake phase as a boundary condition in the program. However, it is not always possible to set up this experimental arrangement. In this study, a setup similar to the experimental measurement technique has been created using ANSYS Design Modeler and CFX to determine the swirl ratio, which is necessarily defined in any combustion analysis.

2.2.1. Boundary conditions

The exhaust ports and valves were removed from the flow volume before starting the analyses, which resulted in a solid geometry with an intake port, as shown in Figure 4. The geometry of the piston is designed in a flat cylindrical shape. The cylinder diameter is realistically set at 104 mm, while the stroke length is extended from 115 mm to 200 mm to measure the swirl intensity at the desired point, minimizing the effect of the outlet boundary condition on the solution. Since a movable mesh structure will not be used, geometries have been separately created for various valve openings ranging from 1 mm to 5.85 mm. For the inlet boundary condition, velocity values

obtained from the 1-dimensional AVL Boost program for different valve openings were used, while the outlet boundary condition was defined as "pressure outlet (atmospheric)," as given in Figure 4.

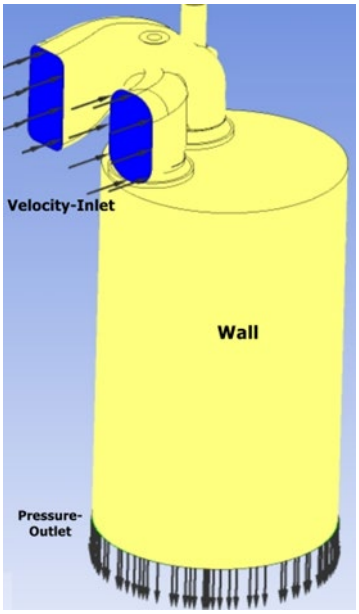

Figure 4. The internal flow volume and boundary condition definitions

Other assumptions made for the numerical analyses are listed below:

- During the intake process, the pressure drop in the intake manifold is assumed to be constant.
- Residual gases from the previous combustion process are not included in the calculations.
- The fluid is chosen as air, assuming it to be an ideal gas.
- The turbulence model is selected as standard k-ε model, and analyses have been repeated for different turbulence models thereafter.
- The analyses are conducted in a steady state.
- Energy equations have not been solved since heat transfer is neglected.

2.2.2. Grid generation

After the creation of the flow volume for the solution step, studies on the sufficient number of elements were conducted to minimize errors arising from the numerical mesh. Structures were examined using tetrahedral elements with approximately 2 million (coarse), 5 million (medium), and 8 million (fine) elements.

The cross-sectional view of the medium-density mesh structure created for maximum valve opening is as shown in Figure 5.

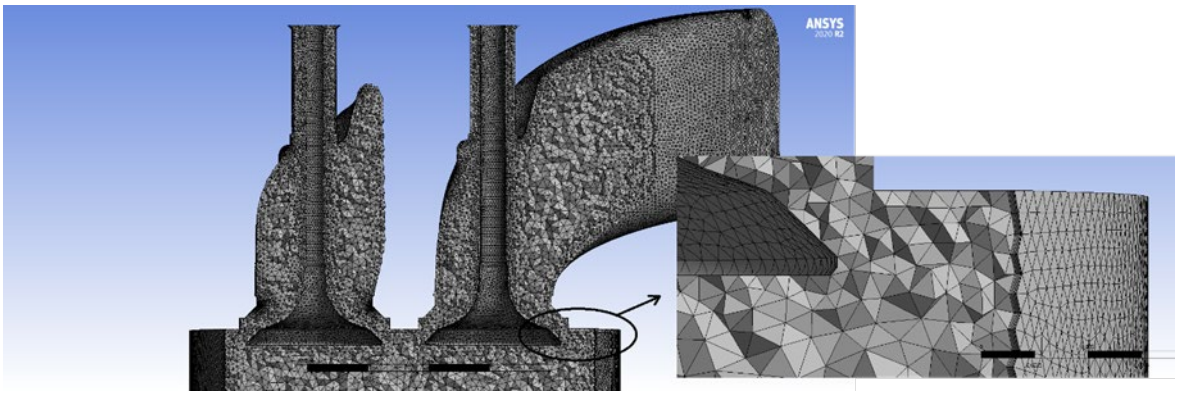

Figure 5. The cross-sectional view of the sample mesh structure for maximum valve opening (5.85 mm) – for medium-density mesh structure

3. FINDINGS AND DISCUSSION

3.1. Mesh Independency

To assess the independence of the obtained results from the solution mesh, tangential velocity measurements were conducted at three different points along the cylinder axis (valve seat - 5 mm, cylinder middle - 60 mm, and cylinder outlet - 120 mm) for three different elements counts at maximum valve lift (5.85 mm), as shown in Figure 6. The variations are presented in Table 1.

Table 1. Variation of velocity at different points along the cylinder axis for different element numbers

Element Number	Velocity – Point 1 (m/s)	Velocity – Point 2 (m/s)	Velocity – Point 3 (m/s)	Swirl Ratio
2,021,072 (Coarse)	98.72	36.46	30.31	0.248
4,954,434 (Medium)	111.7	53.16	34.37	0.236
8,102,462 (Fine)	114.57	59.88	37.19	0.236

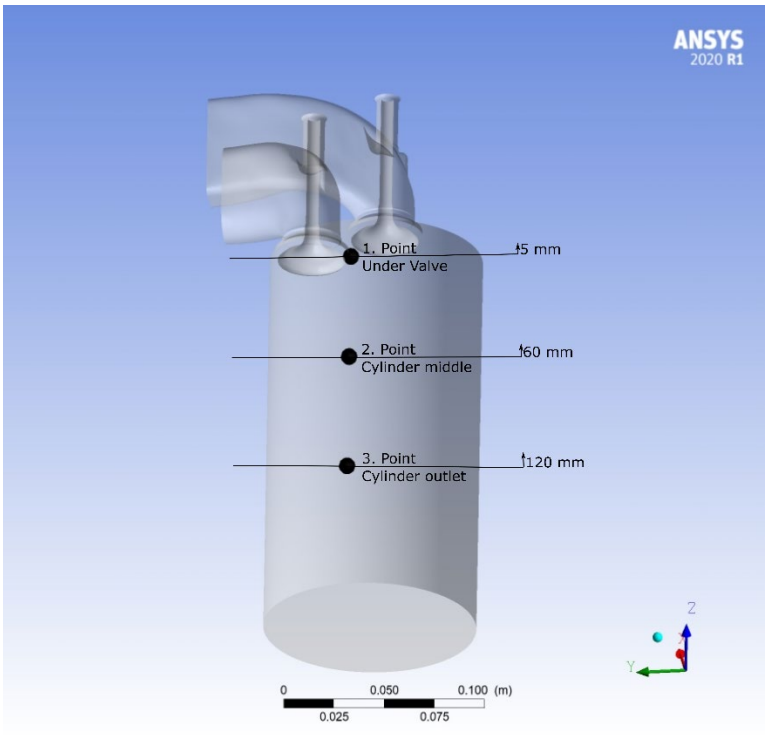

Figure 6. The measurement points used to check independency from the number of elements

Table 1 shows that the maximum difference between the coarse and fine mesh structures is 64.23%, measured at the second point, while the average difference for these three points is 34.32%. Similarly, the maximum difference between the medium and fine mesh structures is observed to be 12.64% at the second point, with the average difference being approximately 7.8%. Similar to the velocity distribution in Table 1, a comparison of tangential velocity has been conducted for three different meshes based on position along the cylinder diameter. Here, it can be observed that the maximum difference between the coarse and fine mesh structures is 66%, while the difference between the medium and fine meshes is around 40%. Additionally, when the swirl ratios based on the position of the planes are compared, a difference of approximately 25% is observed between the fine and coarse mesh structures, while the difference between the medium and fine meshes is calculated to be around 7.5%. As a summary, when Table 1 and Figure 7 are examined together, it is observed that fine and medium mesh structures yield generally very similar results, which leads to the utilization of the medium-density mesh structure in order to reduce computational effort. The swirl ratio used in Table 1 was subsequently calculated using Equation 7 by defining a "field function" in the CFX solver. Additionally, an Excel file was created to obtain position and velocity information for approximately 15,000 points in x, y, and z directions, which was then substituted into Equation 7 for verification.

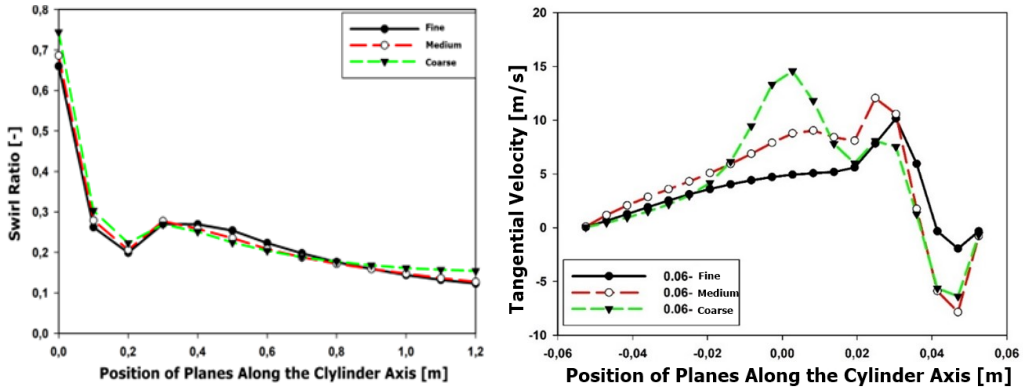

Figure 7. Variation of swirl ratio along different planes along the cylinder axis and tangential velocity change at a valve opening of 5.85 mm across the cylinder diameter. (The middle of the cylinder – having a distance of 60 mm)

3.2. Turbulence Model

After determining the appropriate mesh structure and number of elements, the suitability of the turbulence model was assessed by examining the variation of swirl ratios along different planes along the cylinder axis for the four turbulence models available in ANSYS CFX, as shown in Figure 8.

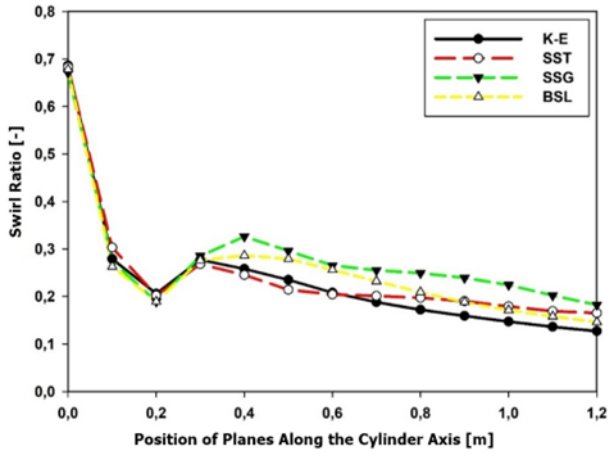

Figure 8. Variation of swirl ratio along the cylinder axis across different planes according to the turbulence models

The k-ε and k-ω models connect Reynolds stresses to mean velocity gradients and turbulent viscosity using gradient diffusion concept. Turbulent viscosity is expressed as a function of turbulent velocity and length scale. In two-equation turbulence models, the turbulent velocity scale is derived using the turbulent kinetic energy acquired from the transport equation's solution. The

turbulent length scale is computed using two turbulence field characteristics: turbulent kinetic energy and convective velocity. The convective velocity of turbulent kinetic energy is obtained from the solution of the transport equation. In general, the k-ω SST model accounts for the transport of turbulent shear stress and provides highly accurate predictions regarding the amount and onset of flow separation under adverse pressure gradients. It is typically used for low Reynolds numbers and values of $y+ < 0.2$ [26]. A review of the literature [27, 28, 29] shows that the k-ε turbulence model provides results closest to experimental data, and therefore, this model has been preferred for the solutions.

3.3. Different Valve Openings

This section explains effects of different valve openings on flow characteristics through contours and graphs. Analyses were conducted in a steady state for valve openings of 1 mm, 2 mm, 3 mm, 4 mm, 5 mm, and the maximum opening of 5.85 mm using approximately 5 million elements and the k-ε turbulence model. For the maximum valve opening, the tangential velocity vectors taken along the horizontal axis at different positions (z = 10 mm, 60 mm, and 120 mm) are shown along with the pressure contours and tangential velocity vectors in the vertical position in Figure 9. The plane created in the vertical position intersects the intake ports and valves. As shown in Figure 9, the velocity increases around the valve due to the narrowing section at the valve openings, creating a swirl flow around the valve. The velocity achieved here is on the order of 106.5 m/s. Additionally, it can be observed that as one moves downward along the vertical axis, the tangential velocity decreases, leading to a corresponding reduction in swirl intensity. When examined the pressure contour along the vertical axis in Figure 9, it can be seen that transient negative pressure formed under the valves contributes to the creation of tumble motion.

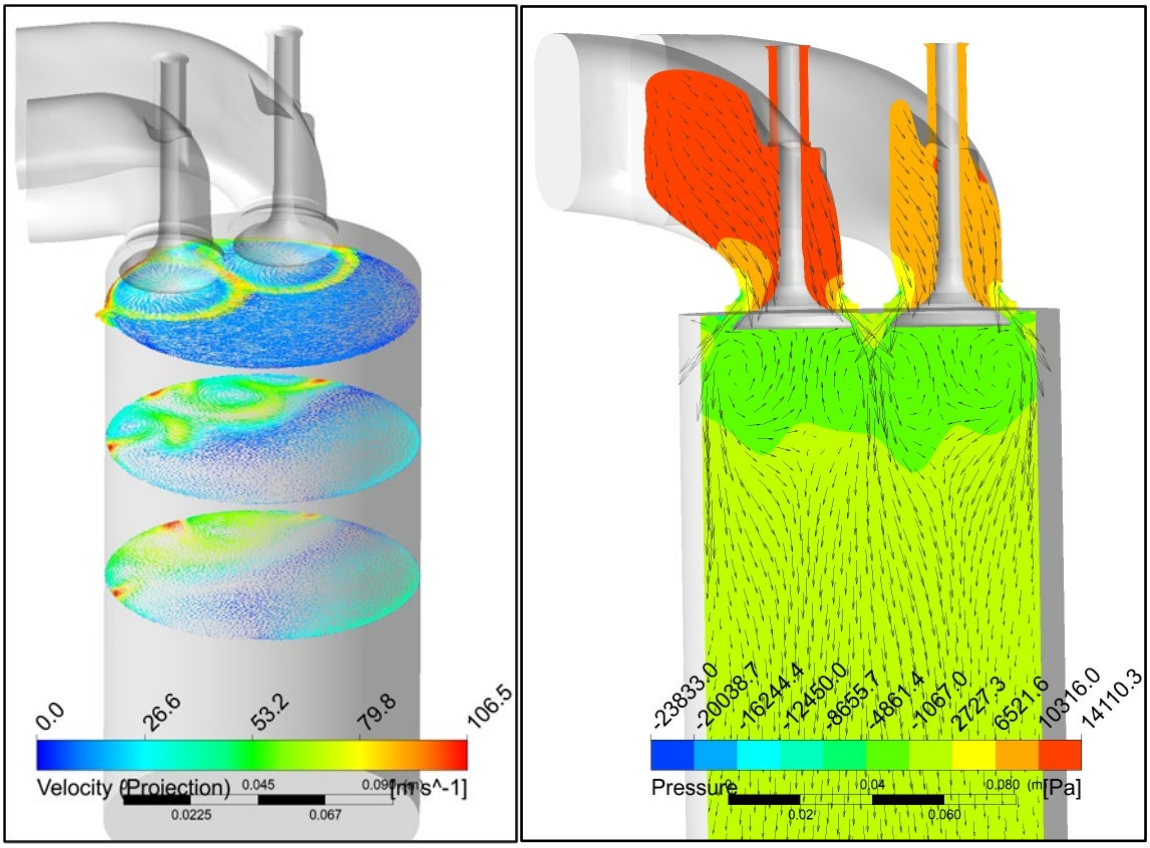

Figure 9. For the maximum valve opening, a) tangential velocity vector distribution and b) pressure contour along the horizontal axis and vertical axis

Valve seating angle, valve structures, and valve openings are also critical variables affecting the mixture quantity within the cylinder. While the valve seating angle and structure of the engine are determined, the effects of different openings on swirl ratio are shown in Figure 10. Generally, it is observed that increasing the valve opening enhances swirl intensity; however, a sudden increase in the swirl ratio is noted at a valve opening of 2 mm. An increase in the swirl ratio up to a certain level enhances turbulence within the cylinder, contributing to improved combustion. The swirl ratio is directly related to the design of the intake manifold and port geometry.

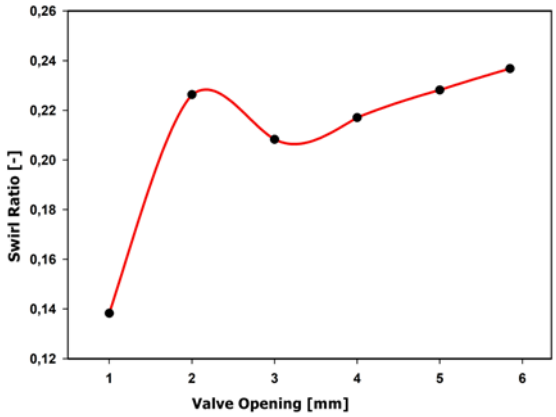

Figure 10. The effect of valve opening on swirl intensity

Upon examining Figure 11, it can be observed that at a valve opening of 5.85 mm, the intensity of the velocity and the number of generated swirls is greater compared to a valve opening of 3 mm. As the valve opening increases, the intensity of cyclicity and tangential velocities also rises, depending on the inlet velocity. This, in turn, leads to an increase in swirl ratio due to the rise in angular momentum. Moreover, when Figures 9 and 11 are examined together, it is observed that the air exhibits a velocity behavior above the inlet speed due to the nozzle effect created by the valve openings. The high velocities generated cause the air to flow through the wall and be directed straightforward to the outlet.

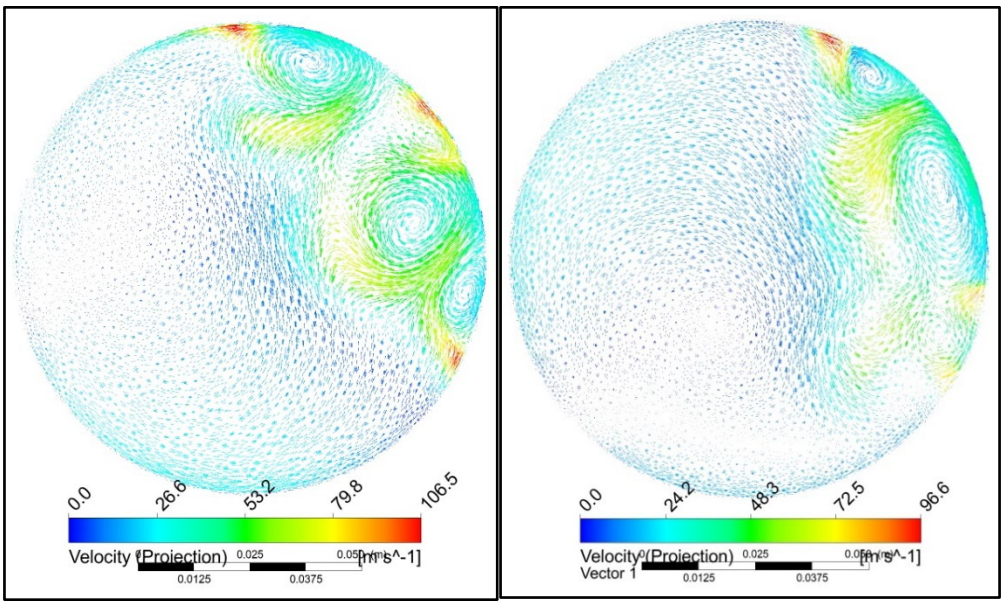

(a) (b)

Figure 11. Tangential velocity vector distribution along the horizontal axis at a valve opening of (a) 5,85 and (b) 3mm (z = 60 mm)

4. CONCLUSIONS AND RECOMMENDATIONS

The presented study focused on the numerical investigation of swirl within a diesel engine under cold starting conditions, examining various valve opening configurations. The findings demonstrate that increased valve openings significantly affect the swirl intensity within the cylinder, which plays a crucial role in improving air-fuel mixing and combustion efficiency. However, the results also highlight that excessive swirl can lead to higher heat transfer rates to the cylinder walls and potential flame propagation issues. The application of computational fluid dynamics (CFD) using the k-ε turbulence model provided reliable predictions that aligned well with experimental data, confirming the model's effectiveness in simulating in-cylinder airflow dynamics. Overall, this research offers valuable insights for optimizing intake port and valve designs to enhance engine performance and reduce emissions, especially under cold start condition.

NOMENCLATURE

m: Mass

ρ: Density

V: Volume

U: Axial velocity

W: Tangential velocity

i,t: Unit vectors

r: Distance

M: Moment of momentum

$\overline{U}, \overline{W}$: Average velocities

u', w': Fluctuations in velocity

M_x: axial moment

$M\varphi$: tangential moment

S: Swirl number

V_θ: tangential velocity (obtained from CFD Analyses)

V_a: axial velocity (obtained from CFD Analyses)

ACKNOWLEDGEMENTS

We would like to express our gratitude to AVL LIST GmbH for providing the AVL Boost software and to Türk Traktör Ziraat Makineleri A.Ş. for supplying the necessary information related to the

engine. This study has been supported by the Scientific Research Projects Coordination Unit of Gazi University under code 06/2019-15.

DECLARATION OF ETHICAL STANDARDS

The authors of the paper submitted declare that nothing which is necessary for achieving the paper requires ethical committee and/or legal-special permissions.

CONTRIBUTION OF THE AUTHORS

Fatih Aktas: Conceptualization, Numerical Analysis, Manuscript Drafting, Manuscript Review, Data Visualization, Manuscript Editing.

Zeynep Aytac Yilmaz: Numerical Analysis, Manuscript Drafting, Manuscript Review, Manuscript Editing.

Nuri Yucel: Conceptualization, Manuscript Review, Manuscript Editing.

CONFLICT OF INTEREST

There is no conflict of interest in this study.

REFERENCES

[1] Taştan M, Mızrak KC. Investigation of propane combustion at different equivalent ratios in a premixed model burner. International Journal of Energy Studies 2023; 8(4): 731-746.

[2] Aktas F. Three-Dimensional Computational Fluid Dynamics Simulation and Mesh Size Effect of the Conversion of a Heavy-Duty Diesel Engine to Spark-Ignition Natural Gas Engine. J. Eng. Gas Turbines Power 2022; 144(6): 061004.

[3] Aktaş F, Yücel N. Dizel bir motorun reaktivite kontrollü sıkıştırma ateşlemeli bir motora dönüşümünde farklı oranlarda propan kullanımının ve yanma başlangıç zamanının performans, emisyon ve silindir içi yanma karakteristiklerine olan etkilerinin incelenmesi. Gazi Üniversitesi Mühendislik Mimarlık Fakültesi Dergisi 2023; 39(2): 785-796.

[4] Aktas F. Numerical investigation of the effect of swirl number on performance, combustion, and emissions characteristics in a converted heavy-duty natural gas engine. Progress in Computational Fluid Dynamics, an International Journal 2024; 24(3): 162-173.

[5] Polat S, Yücesu HS, Kannan K, Uyumaz A, et al. Experimental comparison of different injection timings in an HCCI engine fueled with n-heptane. International Journal of Automotive Science And Technology 2017; 1(1): 1-6.

[6] Temizer İ, Cihan Ö, Öncüoğlu Ö. Numerical investigation of different combustion chamber on flow, combustion characteristics and exhaust emissions. European Mechanical Science 2023; 7(1): 7-15.
[7] Wang Y, Zhang Y, Li Q. An analytic study of applying Miller cycle to reduce NOx emission from petrol engine. Applied Thermal Engineering 2007; 27(11-12): 1779-1789.
[8] Pehlivan EF, Altın İ. A full-scale CFD model of scavenge air inlet temperature on two-stroke marine diesel engine combustion and exhaust emission characteristics. Int J Energy Studies 2024; 9(3): 493-517.
[9] Kethüdaoğlu G, Aktaş F, Karaaslan S, Polat S, Dinler N. Investigation of conversion of a diesel engine to homogeneous charge compression ignition engine using n-heptane: A zero-dimensional modeling. Int J Energy Studies 2023; 8(3): 535-556.
[10] Heywood JB. Internal combustion engine fundamentals. McGraw-Hill Education 2018.
[11] Arcoumanis C, Bicen AF, Vafidis C, Whitelaw JH. Three-dimensional flow field in four-stroke model engines. SAE Technical Paper 1984; 841360.
[12] Arcoumanis C, Bicen AF, Whitelaw JH. Squish and swirl-squish interaction in motored model engines. Journal of Fluids Engineering 1983; 105(1): 105-112.
[13] Demirkesen C, Colak U, Savci IH, Zeren HB. Experimental and numerical investigation of air flow motion in cylinder of heavy-duty diesel engines. Journal of Applied Fluid Mechanics 2020; 13(2): 537-547.
[14] Huang RF, Lin KH, Yeh CN, Lan J. In-cylinder tumble flows and performance of a motorcycle engine with circular and elliptic intake ports. Experiments in Fluids 2009; 46(1): 165-179.
[15] Kaplan M, Özbey M, Özcan H. Numerical investigation of the effects of intake port geometry on in-cylinder motion and combustion in diesel engines. International Journal of Engineering Science 2018; 7: 16-26.
[16] Taghavifar H, Khalilarya S, Jafarmadar S. Engine structure modifications effect on the flow behavior, combustion, and performance characteristics of DI diesel engine. Energy Conversion and Management 2014; 85: 20-32.
[17] Payri F, Benajes J, Margot X, Gil A. CFD modeling of the in-cylinder flow in direct-injection diesel engines. Computers & Fluids 2004; 33(8): 995-1021.
[18] Choi GH, Kim JH, Lee HS, Park SB. A numerical study of the effects of swirl chamber passage hole geometry on the flow characteristics of a swirl chamber type diesel engine.

Proceedings of the Institution of Mechanical Engineers, Part D: Journal of Automobile Engineering 2006; 220(4): 459-470.
[19] Jemni MA, Kantchev G, Abid MS. Influence of intake manifold design on in-cylinder flow and engine performances in a bus diesel engine converted to LPG gas fuelled, using CFD analyses and experimental investigations. Energy 2011; 36(5): 2701-2715.
[20] Shafie NAM, Said MFM. Cold flow analysis on internal combustion engine with different piston bowl configurations. Journal of Engineering Science and Technology 2017; 12(4): 1048-1066.
[21] Wahono B, Setiawan A, Lim O. Experimental study and numerical simulation on in-cylinder flow of small motorcycle engine. Applied Energy 2019; 255: 113863.
[22] Topkaya H, Işık MZ, Çelebi Y, Aydın H. Numerical analysis of various combustion chamber bowl geometries on combustion, performance, and emissions parameters in a diesel engine. International Journal of Automotive Engineering and Technologies 2024; 13(2): 63-72.
[23] Aktas F. Bir dizel motorda çift yakıt olarak propan-dizel kullanımının yanma rejimine, motor performansına ve emisyon değerlerine olan etkilerinin sayısal olarak incelenmesi. PhD thesis, Graduate School of Natural and Applied Sciences, Gazi University 2021.
[24] Crnojevic C, Decool F, Florent P. Swirl measurements in a motor cylinder. Experiments in Fluids 1999; 26(6): 542-548.
[25] FEV Magazine. Customized test bench flow investigation. Retrieved from Online Web Site: https://magazine.fev.com/en/fev-customized-test-bench-flow-investigation/
[26] Ansys, Inc. ANSYS CFX-solver theory guide release 2020-R1. ANSYS, Inc. 2020.
[27] Antila E, Imperato M, Kaario O, Larmi M. Effect of intake channel design to cylinder charge and initial swirl. SAE Technical Paper 2010; 2010-01-0624.
[28] Güney H. Tier IV emisyon seviyesine sahip bir dizel motorun hesaplamalı akışkanlar dinamiği ile akış ve yanma analizi. Master's thesis, TOBB University of Economics and Technology 2014.
[29] Ramajo DE, Nigro NM. In-cylinder flow computational fluid dynamics analysis of a four-valve spark ignition engine: Comparison between steady and dynamic tests. Journal of Engineering for Gas Turbines and Power 2010; 132(5): 1-10.